Ozeren, Yavuz; Altinakar, Mustafa; Wren, Daniel G.

Laboratory Measurements of Dam-Break Flow Using High-Speed Video Capture

LABORATORY MEASUREMENTS OF DAM-BREAK FLOW USING HIGH-SPEED VIDEO CAPTURE

Yavuz Ozeren[1], Mustafa Altinakar[2] and Daniel G. Wren[3]

ABSTRACT

New generation two dimensional models for dam-break flood simulation implement internal boundary conditions to represent various types of terrain and constructed features, such as road and railroad embankments, tunnels, bridges, buildings, etc. There is a lack of experimental data needed to develop and validate these internal boundary conditions; therefore, a multi-purpose experimental facility was designed and constructed to perform channelized and non-channelized dam-break experiments with various types of terrain features. The experimental facility consists of a 3.7 m wide and 7.6 m long tilting platform. Along the lengthwise direction, the upper 2.9 m-long portion of the platform is a tank with sidewalls 0.61 m high that represents the reservoir impounded by a dam. The remaining 4.3 m long lower portion represents the floodplain where various types of flow configurations can be easily set-up. A sliding gate centered in the wall between the reservoir and the floodplain can be rapidly raised to simulate dam failure. The flexible design allows experiments to study unsteady flow over, under and through various types of terrain features under channelized and non-channelized flow conditions. High-speed cameras and acoustic sensors were used to measure the position of the free surface. The three-dimensional time-dependent free surface of the flowing fluid was reconstructed using a pattern projection technique. This paper describes the design, installation, and operation of this multi-purpose dam-break experimental facility. Preliminary results, consisting of three-dimensional water surface elevations are included for a free release from the gate and for flood flow impacting an obstacle oriented transverse to the flow.

1. INTRODUCTION

Dam failures can cause significant loss of life and property damage, especially in highly populated areas. Urban development and land-use on floodplains have increased the severity of the damage bringing more attention to the researchers in recent years. Shallow water equations are commonly used in numerical models to describe strongly unsteady flows like dam-break scenarios (Toro, 2001). Several assumptions are made in the derivation of these models. For example, the flow conditions during the initial stages of a dam break are highly unsteady and local vertical gradients

[1] Research Scientist, NCCHE, National Center for Computational Hydroscience and Engineering, University of Mississippi, Oxford, MS, USA (yozeren@ncche.olemiss.edu)
[2] Director and Research Professor, NCCHE, National Center for Computational Hydroscience and Engineering, University of Mississippi, Oxford, MS, USA (altinakar@ncche.olemiss.edu)
[3] Research Hydraulic Engineer, United States Department of Agriculture, Agricultural Research Service, National Sedimentation Laboratory, Oxford, MS, USA (Daniel.Wren@ars.usda.gov)

can be important around structures, which cannot be resolved by the shallow water equations. The use of a regular rectangular computational mesh offers several advantages in two-dimensional flood simulations and can significantly reduce the computational time. However, certain linear terrain features, such as road and railroad embankments, bridges, culverts, etc., may not be adequately resolved depending on the mesh size. Modern numerical models for dam-break flood analysis use advanced techniques such as internal boundary conditions to correctly represent these features (Altinakar et. al. 2009). It is necessary to test the validity of the assumptions and techniques as well as the reliability and performance of the numerical models. Numerous dam-break experiments have been conducted and reported in the literature (Lauber and Hager, 1998, Cochard and Ancey, 2008, Spinewine and Zech, 2010). Yet, there is still a lack of laboratory and field data that can be used to validate specific features like internal boundary conditions.

The main goal of the current work was to design and construct a multipurpose experimental facility equipped with a very fast opening gate that is able to create an almost ideal dam beak flow. A specific objective was to produce laboratory data sets that can be used to verify and validate the specific features used in numerical models. Here, the experimental procedures and measurement techniques for idealized dam-break simulations are described.

2. MATERIALS AND METHODS

2.1 Test Basin

The experimental facility consists of a 7.6 m-long and 3.7 m-wide platform supported by a structural frame (Figure 1). The platform can be tilted up to a 1:7 positive slope by two powered machine screw jacks mounted on the upstream end of the frame. A 3.2 m-long, 3.5 m-wide, 0.6 m-high reservoir was constructed at one end of the platform and the remaining 4.4 m-long section served as the downstream floodplain. One of the sidewalls of the reservoir was constructed out of 1-inch thick clear acrylic, while the remaining walls were made out of aluminum plate and coated with epoxy. The floodplain floor was constructed ¾” think PVC sheet and coated with matte gray paint. The water spilling off the floodplain was collected by a channel network that led to a sump under the platform, which allowed the water to be recirculated by pumping it back to the test basin reservoir.

On the wall separating the reservoir from the floodplain, a 0.5 m-wide lightweight aluminum gate was installed. The gate was operated by a computer-controlled weight dropping mechanism, which was able to pull the gate at speeds up to 9 m/s. To provide the necessary velocity and acceleration, a 53 kg cylindrical weight was raised by an electromagnetic lifter and dropped at a certain height onto a steel lever that was attached to the gate by a cable and pulley system. The gate was slowed by a pneumatic cylinder mounted along the liner guide that secured the gate in place. The structure that held the gate in place and the linear guide and the pulley system were mounted on a steel frame that was completely separated from the testing platform in order to reduce the dynamic loading on the channel and unwanted disturbances during the experiments. The gate was sealed by a rubber foam gasket at the bottom and high vacuum grease on both sides. The cameras, lights and projectors were held in place by an aluminum structural frame assembly 3.5 m above the floodplain.

(a)

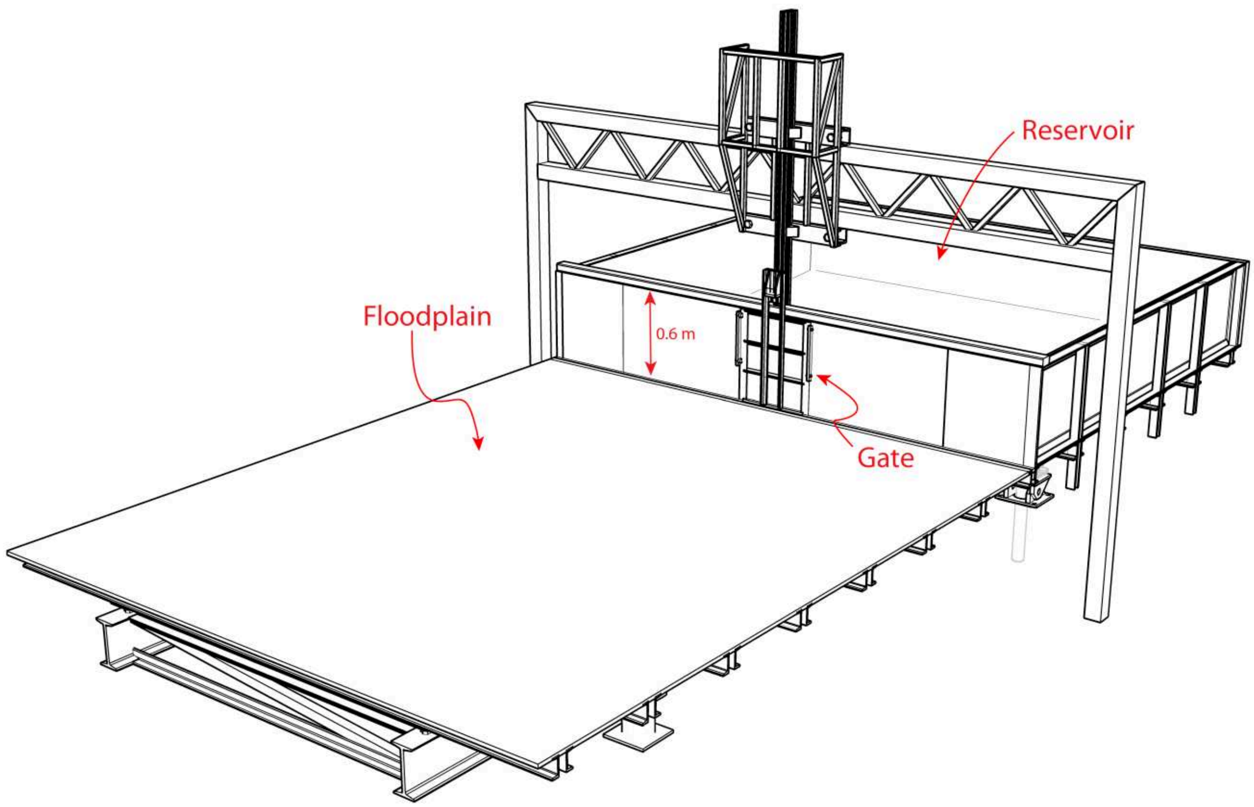

(b)

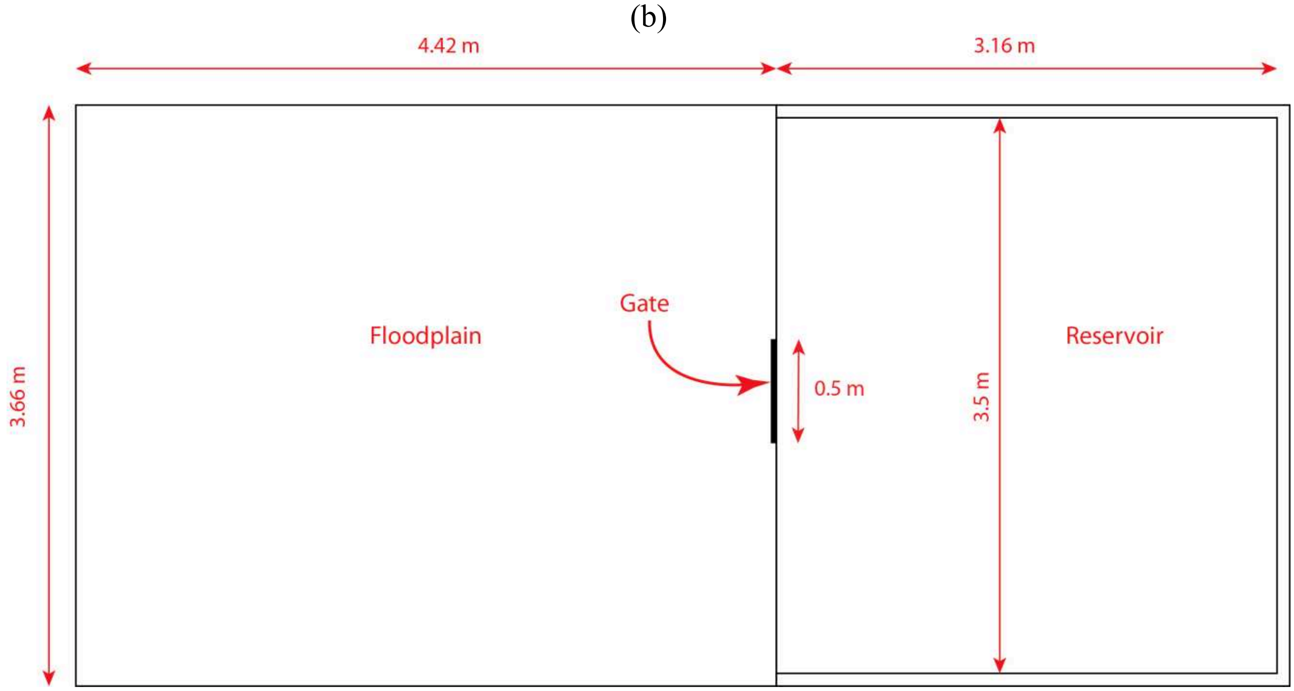

Figure 1 (a) General layout and (b) plan view of the testing platform.

2.2 Experimental Procedure

Prior to each experiment the gate was cleaned up and sealed by vacuum grease. Then, the reservoir was filled up and left to settle down long enough for the circulations to dissipate. Meanwhile, the floodplain was dried and cleaned of any water or debris. The cameras, lights and the instruments were adjusted. Six high speed cameras were positioned at various locations above and around the floodplain with proper lighting conditions. Upon removal of the gate the cameras and the sensors were triggered with a suitable delay based on the distance from the gate in order to maximize the recording time. Figure 2 shows captured images at the overhead, front and side cameras for a typical experiment with a reservoir water depth of h = 0.4 m.

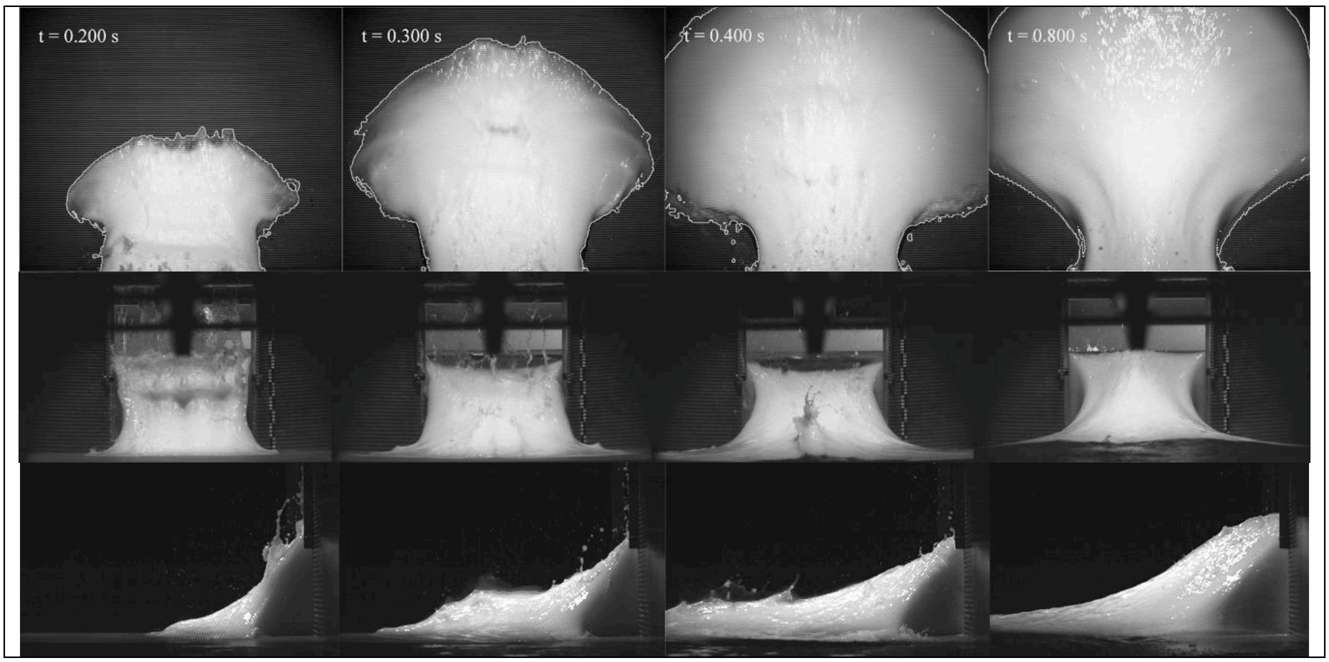

Figure 2 Top, front and side views of a typical gate opening (Reservoir water depth, h = 40 cm).

2.3 Measurement Techniques

Tracking and measurement of the water surface during dam-break experiments is a challenging problem due to the rapidly varying flow conditions. The measurement technique has to be fast and non-intrusive in order to avoid disturbing the flow. Three-dimensional reconstruction techniques based on fringe pattern projection are widely used in various fields such as remote sensing, industrial monitoring and biomedicine (Su and Zhang, 2010). The most common technique is projection of a Ronchi pattern, which is a series of alternating shadow lines, onto a surface. Then, elevations are extracted by comparing the deformed and non-deformed grating. Fourier transform profilometry (FTP), introduced by Takeda et. al. (1982), is a common method used to extract the phase information using Fast Fourier Transforms. In this study, free surface displacement was measured by phase profilometry in addition to acoustic and capacitance sensors. Five ultrasonic transducers and two capacitance water level sensors were used to measure the free surface elevation. The acoustic sensors were hung by steel strings from the overhead frame and stabilized by adding weights to ensure that vibrations didn't interfere with the instruments. The capacitance sensors were used on the reservoir side and were mounted on the reservoir walls. Preliminary experiments showed that the repeatability was very good between independent runs. Therefore, the acoustic sensors were repositioned between runs to increase the number of measurement points. The capacitance sensors were kept fixed in place for reference.

2.4 Phase Profilometry

A Ronchi fringe pattern with a known line frequency was projected onto the water surface by a slide projector positioned 3.17 m above the floodplain illuminating an area approximately 1 m x 1 m. A high-speed camera was mounted at the same height with the projector to capture the reflected fringes. To increase opacity and reflection from the water surface, a mixture of titanium dioxide (TiO_2) and fluorescent green water dye was added into the water. The dye also provided contrast between the water and flood plan floor and enabled tracking of the wave front. Figure 3a shows the projected fringe pattern over the water surface for a typical experiment. The optical geometry of the fringe projection and imaging system is described in Figure 3b. The camera and the projector are arranged in such a way that their lenses are at the same height, l_o, from the reference plane (the floodplain on the test basin) and with a distance λ between them. The optical axis of the camera and projector were on the same plane, which was perpendicular to the floodplain. Depending on the free surface topography, the fringe pattern deformed creating a phase shift $\varphi(x,y)$ relative to the undistorted fringe (Takeda et al., 1982). The elevation of the free surface relative to the reference plane can be obtained from the geometric similarity by:

$$\eta(x,y) = \frac{l_0 \varphi(x,y)}{\varphi(x,y) - 2\pi\lambda f_0} \tag{1}$$

where f_0 is the spatial-carrier frequency of the fringe pattern. The light intensity I*(x,y)* of a given point on the floodplain from the camera point of view can be written as:

$$I(x,y) = a(x,y) + b(x,y)\cos[2\pi f_0 x + \varphi(x,y)] \tag{2}$$

where, *a(x,y)* is the background intensity, *b(x,y)* is the background modulation or,

$$I(x,y) = a(x,y) + c(x,y)\exp(2\pi i f_0 x) + c^*(x,y)\exp(-2\pi i f_0 x) \tag{3}$$

where $i = \sqrt{-1}$ and,

$$c(x,y) = \frac{1}{2} b(x,y)\exp(i\varphi(x,y)) \tag{4}$$

The two-dimensional Fourier transform of Eq. 3 can written as

$$G(f,g) = A(f,g) + C(f - f_0, g - g_0) + C(f + f_0, g + g_0) \tag{5}$$

where f and g are the frequencies in the x and y directions and capital letters denote Fourier spectra. If the spatial variations of *a(x,y)* and *b(x,y)* are small the compared to f_0, one of the fundamental components can be filtered out and shifted to the origin. This procedure is illustrated in Figure 4 for a one-dimensional Fourier transform. Figure 5a shows the two-dimensional Fourier spectra for projected fringe pattern.

The filtered spectrum is then transformed back to the spatial domain by two-dimensional inverse Fourier transform. Finally, the complex logarithm of Eq. (4) is calculated in order to separate the phase distribution from the background modulation:

$$\log(c(x,y)) = \log[\frac{1}{2}b(x,y)] + i\varphi(x,y) \tag{6}$$

The imaginary part of Eq. (6) yields the wrapped phase map of the projected fringe pattern, which has values ranging between $-\pi$ to π with discontinuities of 2π phase jumps. Figure 5b shows the wrapped phase map of the floodplain before the gate opening and Figure 5c shows 400 ms after the gate opening. The wrapped phase distribution has to be converted to a continuous phase distribution by a phase-unwrapping method.

(a)

(b)

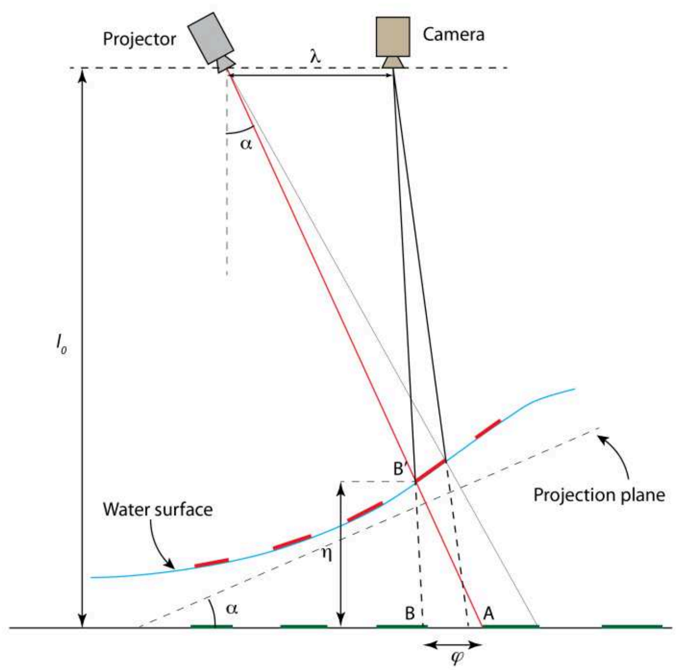

Figure 3 (a) A typical experiment with projected fringe pattern and (b) schematics of the optical geometry for a fringe projection and imaging system.

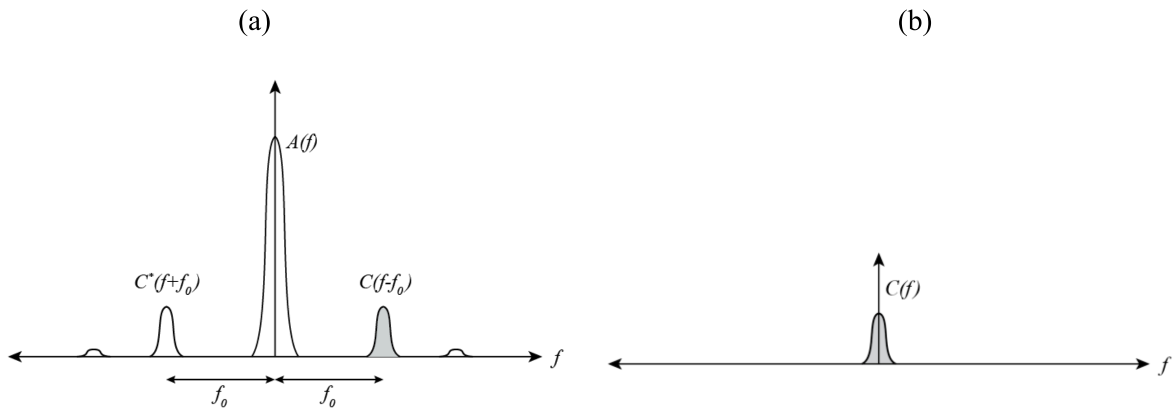

Figure 4 (a)Two sided spectra of a fringe pattern with background gradient, and (b) filtered and translated spectrum.

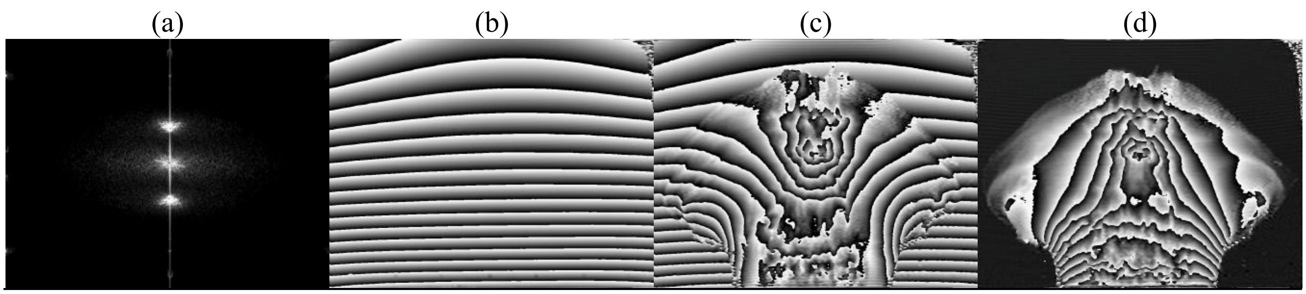

Figure 5 An example of 2D-phase unwrapping (Reservoir water depth, h = 40 cm), (a) 2D Fourier spectrum of the image, (b) phase map of the reference plane, (c) phase map of the free surface and (d) differences of the phase maps in (b) and (c).

Phase unwrapping has been extensively studied and various algorithms have been developed (Ghiglia and Pritt, 1998). The simplest method is one-dimensional phase unwrapping, where each row or column of the wrapped phase map is scanned separately for discontinuities and unwrapped by adding or subtracting 2π according to the phase jump. One-dimensional phase unwrapping is very efficient when the wrapped phase map is noise free and there are no shadows in the original image. First, the discontinuities of the wrapped phase are located by calculating the differences of the consecutive pixels. Next the step differences are converted to binary form and accumulated to obtain the offset phase distribution. Finally, the wrapped phase is multiplied by the offset phase distribution to obtain the unwrapped phase distribution. A row passing close to the center of the wrapped phase map in Figure 5c is used to illustrate the steps in the one-dimensional phase unwrapping procedure in Figure 6. The final step of phase profilometry is converting the computed unwrapped phase map into real coordinates by using Eq. 1.

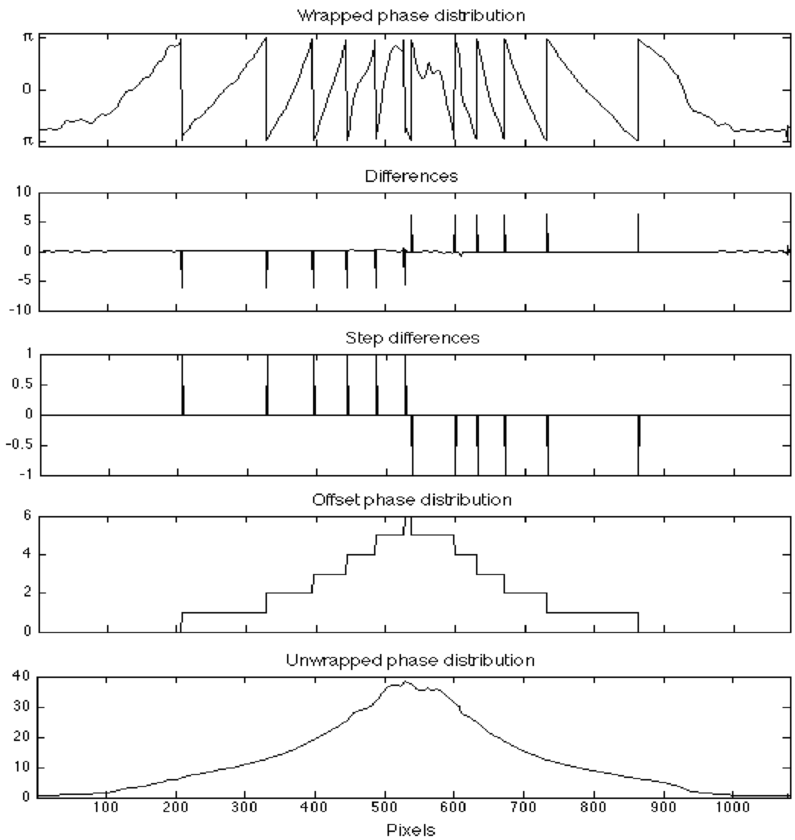

Figure 6 An example of 1D-phase unwrapping (Reservoir water depth, h = 40 cm).

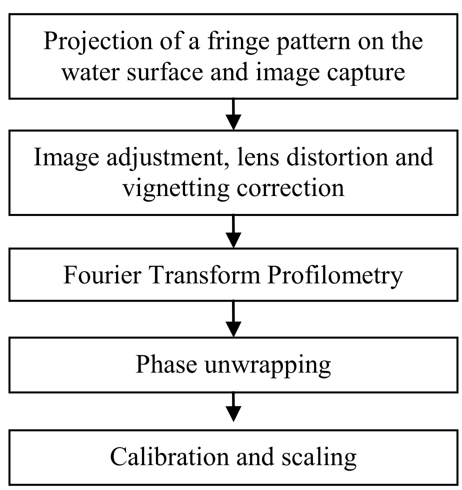

Figure 7 Summary flow chart for phase profilometry.

The major steps of the procedure are summarized in Figure 7. Two of the more challenging steps during the application of the procedure are the projection of a fringe pattern on the water surface and the capturing quality images. For an initial reservoir depth of 0.4m, the theoretical velocity immediately after the sudden removal of the gate is about 4 m/s. Thus, it only takes 0.25 s for the front of the flow to cross the entire projection area. Therefore, high-speed cameras are necessary to for capturing the flow surface. Increasing the frame rate and shutter speed of the camera reduces the exposure time and increases the requirement for light. Consumer grade digital projectors can provide about 5,000 lumens, but they use micro mirror technology that generally has a 120Hz refresh rate which creates flickering in the recorded videos. In this study, conventional slide projectors were used to provide continuous light.

2.3 Interface Tracking

A camera was placed on one side of the floodplain in addition to the overhead camera to capture the dam-break wave from the side. The optical axis of the camera was aligned parallel to the floodplain and perpendicular to the flow direction (x-axis). A checkerboard pattern with known properties was used for image calibration. Six 750-watt HPL tungsten lights with PAR housings were used to illuminate the free surface. Diffuser panels were used to eliminate shadows and reflection over the water surface and create an even light distribution. In some experiments, the slide projector was used to illuminate only one half of the floodplain along the centerline in the direction of the flow. This way, it was possible to capture the water surface profile along the axis of symmetry.

Each image was corrected for lens distortion, cropped around the area to be analyzed, and converted to 8 bit grayscale. The first frame, which was shot before the gate removal, was subtracted from the remaining frames to eliminate background modulation and to increase the contrast. Then, each image was converted to a binary image. The free surface interface was estimated by an edge detection algorithm. The estimate free surface was translated into real coordinates according to the predicted calibration values.

3. RESULTS

The results of two test cases are presented to demonstrate the capabilities of the equipment and procedures described in the previous sections. The first case is a simple dam break flow with a reservoir water depth of 0.3 m. A 25 lines/inch Ronchi pattern was projected on the floodplain surface to produce 24 pixel wide lines on the captured images. The overhead high-speed camera recorded at 200 fps with a resolution of 900x900 pixels covering approximately 1.2 m x 1.2 m square. Figure 8 show the measured water surface profiles at t = 0.2 s, 0.4 s, 1.0 s and 2.0 s. The origin is at the center of the gate on the floodplain level, with the downstream direction being *x*-positive. The colors indicate depth contours, with dark red at the highest elevations and dark blue at the lowest. In Figure 9a, the detected free surface interface is overlaid on the image and in Figure 9b the scaled water surface profiles along the centerline are plotted at t = 0.2 s, 0.4 s, 1.0 s and 2.0 s.

The second example is the dam-break flood interacting with a simple obstacle on the floodplain (Figure 10). A 42 cm long, 10 cm high, 0.5 cm thick clear Lexan plate was attached to the floor perpendicular to the flow direction (aligned with the *y*-axis) and 3.2 m downstream of the gate. The water level at the reservoir was again 0.3 m. A camera was positioned 3.17 m above the obstacle. The camera axis was perpendicular to the floor and crossed the floor 10 cm upstream of the center of the obstacle. A 25 lines/inch Ronchi pattern was used for phase profilometry. Figure 10 shows the greyscale images used for the analysis and the estimated free surface elevations contours of the scaled image.

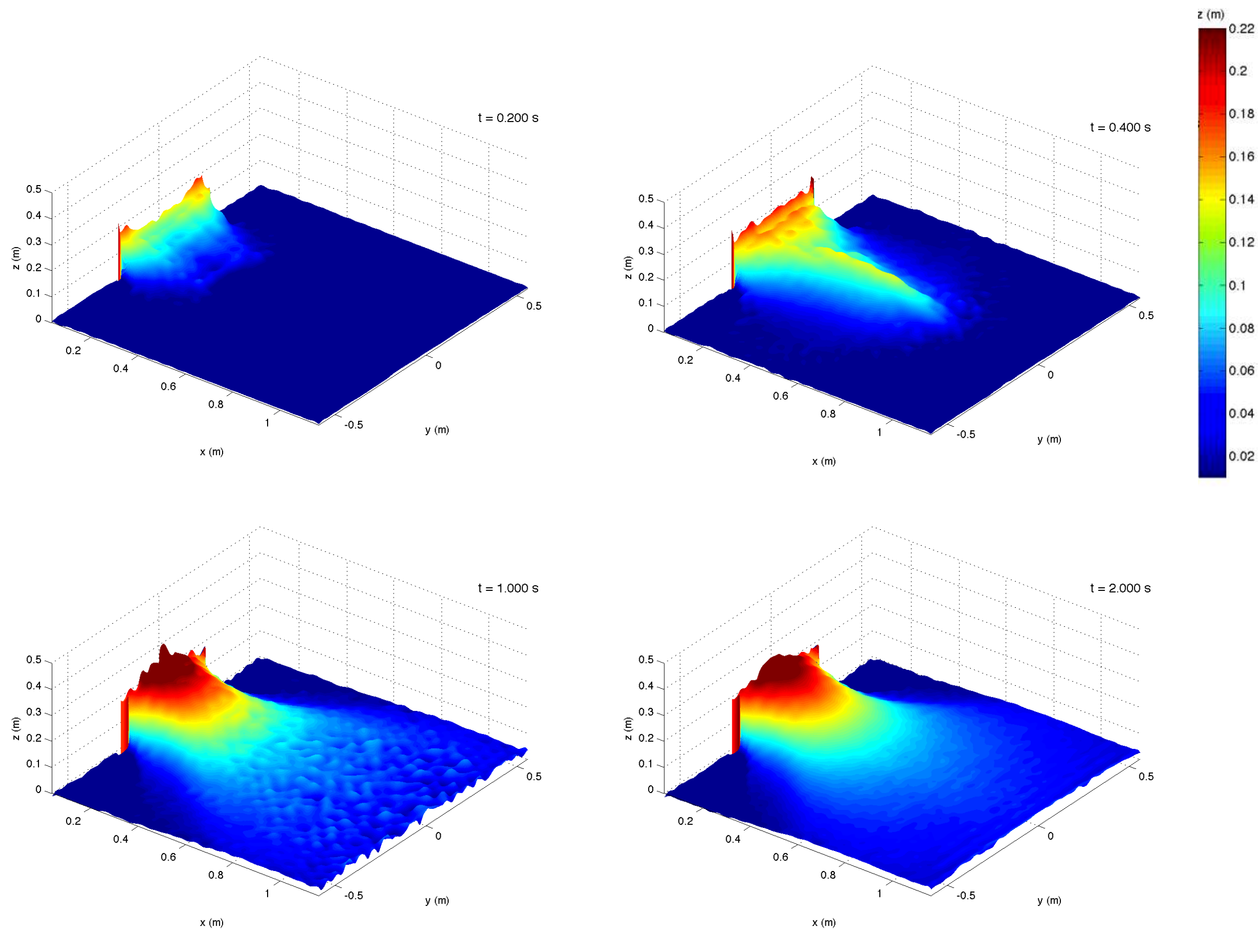

Figure 8 Unwrapped and scaled water surface profiles (Reservoir water depth, h = 30 cm).

(a)

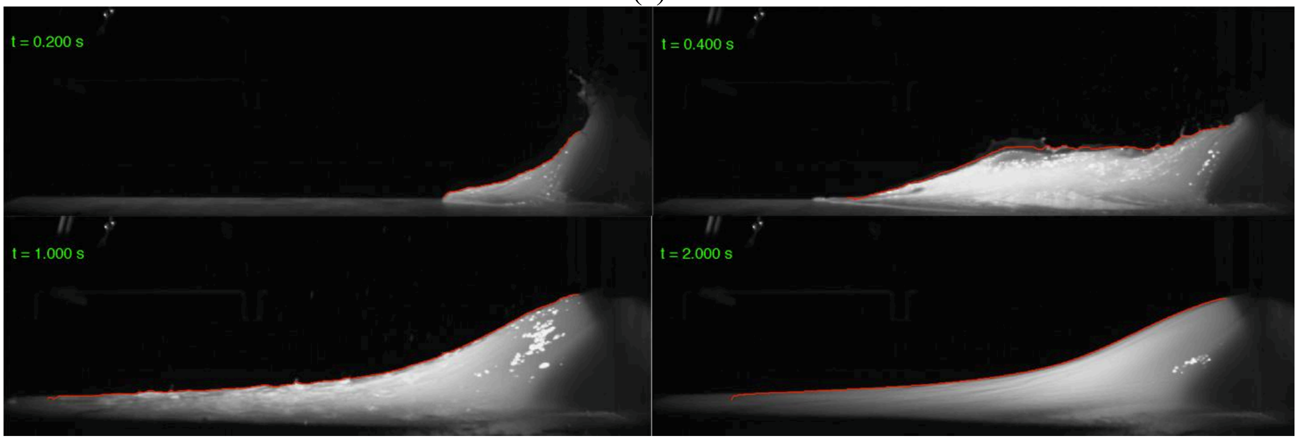

(b)

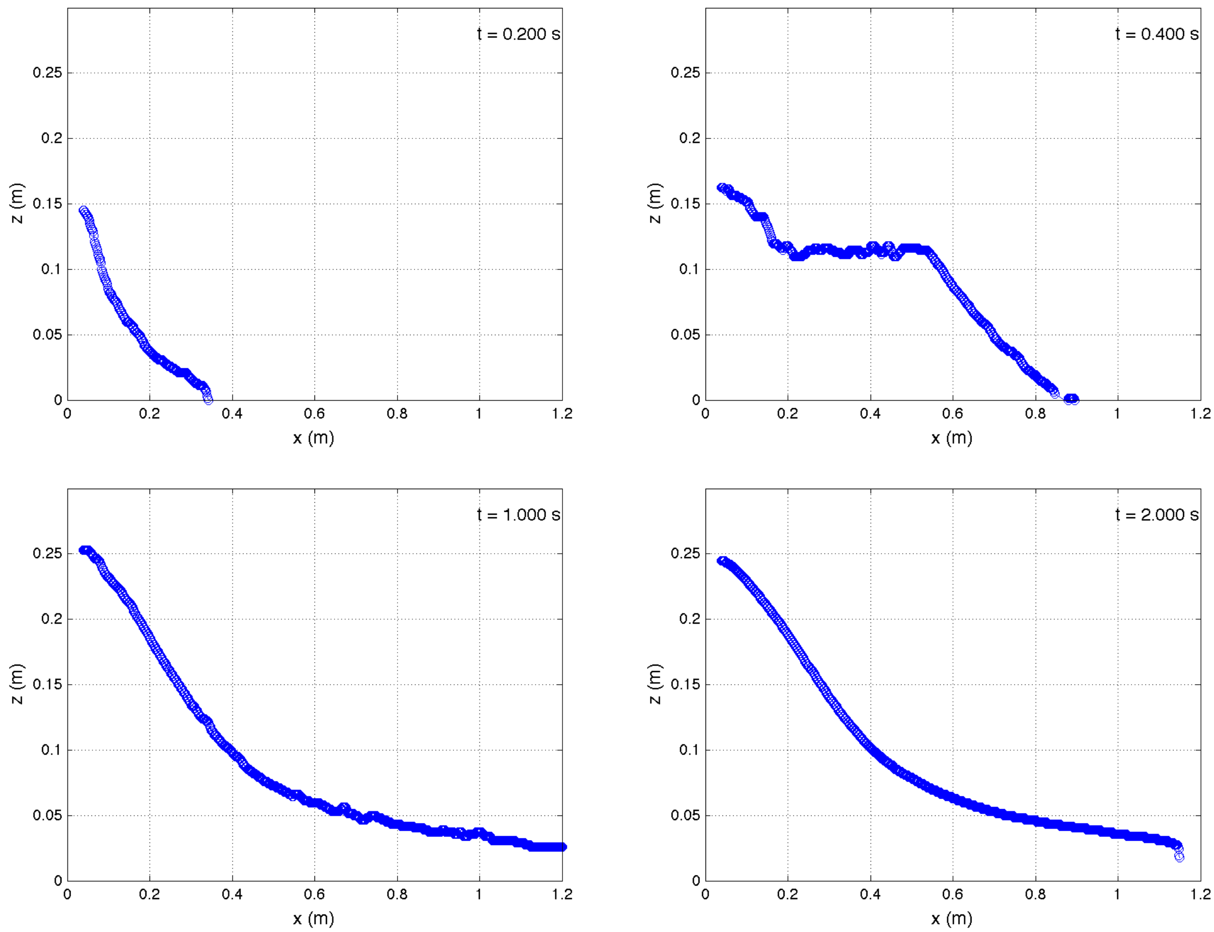

Figure 9 (a) Detected free surface and overlaid on the image and (b) the scaled water surface profile along the centerline (Reservoir water depth, h = 30 cm).

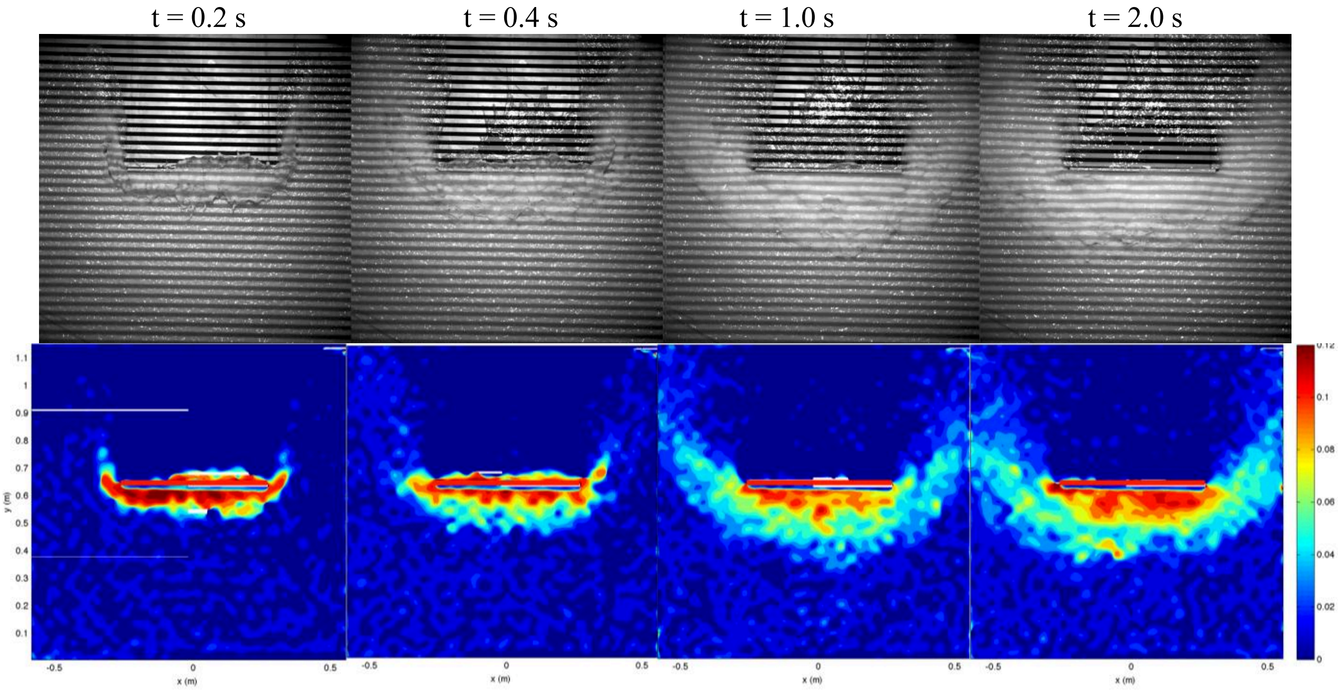

Figure 10 Dam-break flood impacting transverse obstacle (Reservoir water depth, *h* = 30 cm).

3. CONCLUSION

A comprehensive experimental facility designed to support numerical modeling of dam-break events was presented. The design of the structure, data collection procedures, and image analysis techniques were presented, along with results from experiments. Two- and three-dimensional free surface profiles were captured using a high-speed digital camera coupled with the projection of a suitable light/dark grid. Based on the work described here, it can be concluded that the use of high speed cameras can be effective for capturing the transient flow aspects of a progressing flood wave with 4 mm vertical 1.3 mm horizontal resolution over 1.2 m x 1.2 m area. This system was also effective at capturing the topography of flow caused by impacting an obstacle.
The system can be to capture flows over larger areas by integrating multiples camera-projector couples. The system can further be improved by using finer Ronchi patters. An in depth verification and validation analysis is necessary to test the reliability the method.

ACKNOWLEDGEMENTS

This research was supported by the US Department of Homeland Security-sponsored Southeast Region Research Initiative (SERRI) at the US Department of Energy's Oak Ridge National Laboratory. Jacob Ferguson and Alan Barger provided highly capable technical support during the construction and data collection phases of this work. Glenn Gray provided purchasing and logistical support that was integral to the successful progress of this project.

REFERENCES

Lauber, G. and Hager, W. H. 1998. "Experiments to Dambreak Wave: Sloping Channel." *Journal of Hydraulic Research* 36 (5): 761-772.

Cochard, S. and Ancey, C. 2008. "Tracking the Free Surface of Time-Dependent Flows: Image Processing for the Dam-Break Problem." *Experiments in Fluids* 44 (1): 59-71.

Spinewine, B., and Zech, Y. 2007. "Small-Scale Laboratory Dam-Break Waves on Movable Beds." *Journal of Hydraulic Research* 45 (SPEC. ISS.): 73-86.

Su, X. and Q. Zhang. 2010. "Dynamic 3-D Shape Measurement Method: A Review." *Optics and Lasers in Engineering* 48 (2): 191-204.

Takeda, M., Ina, H., and Kobayashi, S. 1982. "Fourier-Transform Method of Fringe-Pattern Analysis for Computer-Based Topography and Inteferometry." *Journal of the Optical Society of America* 72 (1): 156-160.

Ghiglia DC and Pritt MP (1998) *Two-dimensional phase unwrapping: theory, algorithms, and software*. Wiley-Interscience, Wiley, cop.

Altinakar, M.S., M.Z. McGrath, Y. Ozeren and E. Miglio, 2009. “Two-Sided Cut-Cell Boundary Method for Simulating Linear Terrain features and 1D Stream Flows on a 2D Rectangular Mesh”, *Proceedings of the 33rd International IAHR Biennial Congress*, Vancouver, Canada.

Cox, C., McCleave, B., Welch, C.R., Seabergh, W. & Curtis, W. 2001, "Phase profilometry measurement of wave field histories", *Proceedings of the International Symposium on Ocean Wave Measurement and Analysis*, pp. 268.

Toro, E. F., 2001. *Shock-Capturing Methods for Free-Surface Shallow Flows*, John Wiley & Sons, New York/Chichester